Marmoset Serotonin 5-HT 1A Receptor Mapping with a Biased Agonist PET Probe 18 F-F13714: Comparison with an Antagonist Tracer 18 F-MPPF in Awake and Anesthetized States

Chihiro Yokoyama, Aya Mawatari, Akihiro Kawasaki, Chiho Takeda, Kayo Onoe, Hisashi Doi, Adrian Newman-Tancredi, Luc Zimmer, Hirotaka Onoe

OXFORD

International Journal of Neuropsychopharmacology (2016) 00(00): 1–12

doi:10.1093/ijnp/pyw079
Advance Access Publication: September 08, 2016
Regular Research Article

REGULAR RESEARCH ARTICLE

Marmoset Serotonin 5-HT$_{1A}$ Receptor Mapping with a Biased Agonist PET Probe ^{18}F-F13714: Comparison with an Antagonist Tracer ^{18}F-MPPF in Awake and Anesthetized States

Chihiro Yokoyama, MD, PhD; Aya Mawatari, MSc; Akihiro Kawasaki, MA; Chiho Takeda, MA; Kayo Onoe, MA; Hisashi Doi, PhD; Adrian Newman-Tancredi, PhD; Luc Zimmer, PharmD, PhD; Hirotaka Onoe, PhD

RIKEN Center for Life Science Technologies, Kobe, Hyogo, Japan (Dr Yokoyama, Ms Mawatari, Mr Kawasaki, Ms Takeda, Ms K. Onoe, Dr Doi, Dr H. Onoe); Neurolixis Inc, Dana Point, CA (Dr Newman-Tancredi); Université Claude Bernard Lyon 1, Hospices Civils de Lyon, INSERM, CNRS, Lyon Neuroscience Research Center, Lyon, France (Dr Zimmer).

Correspondence: Hirotaka Onoe, PhD, RIKEN Center for Life Science Technologies, 6-7-3 Minatojima Minamimach, Chuo-ku, Kobe, Hyogo 650-0047, Japan (hiro.onoe@riken.jp).

Abstract

Background: In vivo mapping by positron emission tomography of the serotonin 1A receptors has been hindered by the lack of suitable agonist positron emission tomography probes. ^{18}F-labeled F13714 is a recently developed biased agonist positron emission tomography probe that preferentially targets subpopulations of serotonin 1A receptors in their "active state," but its brain labeling pattern in nonhuman primate has not been described. In addition, a potential confound in the translatability of PET data between nonhuman animal and human arise from the use of anesthetics that may modify the binding profiles of target receptors.

Methods: Positron emission tomography scans were conducted in a cohort of common marmosets (n = 4) using the serotonin 1A receptor biased agonist radiotracer, ^{18}F-F13714, compared with a well-characterized ^{18}F-labeled antagonist radiotracer, ^{18}F-MPPF. Experiments on each animal were performed under both consciousness and isoflurane-anesthesia conditions.

Results: ^{18}F-F13714 binding distribution in marmosets by positron emission tomography differs markedly from that of the ^{18}F-MPPF. Whereas ^{18}F-MPPF showed highest binding in hippocampus and amygdala, ^{18}F-F13714 showed highest labeling in other regions, including insular and cingulate cortex, thalamus, raphe, caudate nucleus, and putamen. The binding potential values of ^{18}F-F13714 were about one-third of those observed with ^{18}F-MPPF, with marked individual- and region-specific differences under isoflurane-anesthetized vs conscious conditions.

Conclusions: These findings highlight the importance of investigating the brain imaging of serotonin 1A receptors using agonist probes such as ^{18}F-F13714, which may preferentially target subpopulations of serotonin 1A receptors in specific brain regions of nonhuman primate as a biased agonist.

Keywords: 5-hydroxytryptamine, *Callithrix jacchus*, F13714, biased agonism

Received: June 17, 2016; **Revised:** August 22, 2016; **Accepted:** September 5, 2016

Significance Statement

Serotonin is a neurotransmitter substance in the brain that modulates numerous physiological functions, and the serotonin 1A receptor is a therapeutic target for neuropsychiatric and neurological disorders. Positron emission tomography has been used to characterize the serotonin 1A receptor in living brain, but there is still a lack of suitable agonist probe for studying the functional state of the serotonin 1A receptor. Here, we report the quantitative binding distribution in nonhuman primate brain of ^{18}F-F13714, a recently developed agonist positron emission tomography probe for serotonin 1A receptor, and compare this with a well-characterized antagonist positron emission tomography probe, ^{18}F-MPPF, under both consciousness and isoflurane-anesthesia. ^{18}F-F13714 binding distribution in marmoset monkeys differs markedly from that of ^{18}F-MPPF, with significant individual- and region-specific differences under anesthetized vs conscious conditions. Our findings highlight the importance of investigating the brain imaging of serotonin 1A receptors using agonist probes such as ^{18}F-F13714, which may preferentially target subpopulations of serotonin 1A receptors as a biased agonist.

Introduction

Brain serotonin (5-hydroxytryptamine; 5-HT) is implicated in the control of cognitive and socioemotional abilities in various neuropsychiatric and neurological disorders (Kranz et al., 2010; Kiser et al., 2012; Olivier, 2015). Among the subtypes of 5-HT receptors, the 5-HT$_{1A}$ receptor is most widely distributed in the brain and is a therapeutic target for a variety of CNS disorders (Pazos and Palacios, 1985; Maurel et al., 2007; Celada et al., 2013; Billard et al., 2014 Recently, Lemoine et al. (2012) developed a 5-HT$_{1A}$ receptor agonist PET probe by ^{18}F-labeling of F13714, a highly selective and efficacious 5-HT$_{1A}$ receptor agonist with very high binding affinity (Ki values <0.1 nM) (Koek et al., 2001). F13714 exhibits high selectivity for 5-HT$_{1A}$ receptor in more than 40 other binding sites, including receptors, transporters, ion channels, and enzymes, which were tested by in vitro binding screening assays using both native rat and recombinant human binding sites (Assié et al., 2006) and shows high sensitivity to endogenous agonist, 5-HT, and G-protein uncoupling by Gpp(NH)p in the rat brain (Lemoine et al., 2012). Further, ^{18}F-F13714 rapidly penetrates the blood–brain barrier with high lipophilicity and is only slightly metabolized in vivo (Lemoine et al., 2012). Intriguingly, a PET study using anesthetized cats indicated that ^{18}F-F13714 preferentially binds to cortical rather than hippocampal 5-HT$_{1A}$ receptors, in contrast to findings with antagonist tracers showing a higher density in the hippocampus than in the cortex (Aznavour and Zimmer, 2007; Lemoine et al., 2012). These data reinforce the interpretation that the capacity to label "functional" 5-HT$_{1A}$ receptors may differ substantially between agonist and antagonist radiotracers. In addition, a variety of rat electrophysiological, neurochemical, and behavioral studies have indicated F13714 exhibits a biased agonist profile of activity at specific 5-HT$_{1A}$ receptor subpopulations, notably in the raphe region and the striatum (Newman-Tancredi et al., 2009; Iderberg et al., 2015; van Goethem et al., 2015; de Boer and Newman-Tancredi, 2016). A recent study in phMRI showed that F13714 and another biased agonist, F15599, induced specific pattern of changes in blood oxygen level dependent (BOLD) signal in a neuronal circuit in contrast to those induced by a classical agonist, 8-OH-DPAT, or a silent antagonist, MPPF, supporting the concept that biased agonists can preferentially target subpopulations of 5-HT$_{1A}$ receptors in specific brain regions (Becker et al., 2016). Investigation of brain imaging with ^{18}F-F13714 is therefore desirable to better understand agonist interactions at subpopulations of 5-HT$_{1A}$ receptors.

Although previous experiments have demonstrated the utility of ^{18}F-F13714 as a PET probe for the 5-HT$_{1A}$ receptor in cat (Assié et al., 2006; Maurel et al., 2007; Lemoine et al., 2012), the brain labelling pattern of ^{18}F-F13714 in nonhuman primate has not been described. This would be highly informative, because the translatability of the novel biased agonist profile of F13714 to primate species (and particularly to human) remains to be established. Thus, use of nonhuman primates such as common marmosets, a species that shows human-like sociability involving serotoninergic neurotransmission (Yokoyama et al., 2013), is an attractive option for preclinical PET studies.

A supplementary issue that influences translatability of PET imaging data between animal and human studies is the use of anesthetics that may modify the binding profiles of target receptors (Elfving et al., 2003; Seeman and Kapur, 2003; Lancelot and Zimmer, 2010; Li et al., 2013). Carrying out marmoset PET without anesthesia may therefore be useful for identifying potential confounds in PET imaging due to anesthesia and for mapping the function of serotonin in vivo (Yokoyama et al., 2010; Yokoyama and Onoe, 2015).

The present study therefore had 2 aims. Firstly, to conduct PET scans in a cohort of marmosets using the agonist PET probe, ^{18}F-F13714, and compare this with a well-characterized ^{18}F-labeled antagonist PET probe, ^{18}F-MPPF. Secondly, experiments were performed under both consciousness and isoflurane-anesthesia conditions. This study unveiled a differential binding distribution between agonist and antagonist PET probes, with differential impacts of isoflurane. Thus, the agonist PET probe, ^{18}F-F13714, can provide functional binding profile of 5-HT$_{1A}$ receptors in the primate brain, which will help to further our understanding of the function of serotoninergic system in the human brain and its role in cognitive and socioemotional abilities.

MATERIALS AND METHODS

Subjects

Four adult male common marmosets (*Callithrix jacchus*) (including one pair of siblings), at 3.5 to 4.0 years of age at the start of experiments, were used in these studies. Animals were housed in pairs in home cages measuring 600 × 430 × 650 mm under a 12-h-light/-dark cycle (light: 8:00 AM to 8:00 PM). Each cage had 2 wooden perches, a food tray, and an automatic water dispenser. Animals were fed solid food (CMS-1, CLEA Japan, Inc., Tokyo, Japan) soaked in water and mixed with a suitable amount of powdered milk formula, honey, gluconic acid calcium, vitamin C, and lactobacillus probiotic twice a day, supplemented with chopped boiled eggs or bananas once a week. Each animal underwent PET scans 4 times with ^{18}F-F13714 and ^{18}F-MPPF within 1 year, both under consciousness and isoflurane anesthesia at a 3-week interval.

To perform PET scans on conscious marmosets without causing discomfort to the animals, experiments were conducted

according to a previously published method (Yokoyama et al., 2010). Briefly, animals were adequately trained for fixation on the chair with an acrylic head holder that was surgically attached to the skull surface before PET experiment. For PET scans under anesthesia, animals were maintained with isoflurane inhalation via a mask lying on a bed without the use of a head holder. MRI of the brain was acquired before surgery of the head holder attachment with a 3T MRI scanner (Magnetom Allegra, Siemens, Erlangen, Germany) under pentobarbital anesthetic for the anatomical alignment of PET data. Animals were maintained and handled in accordance with the recommendations of the United States National Institutes of Health, and all procedures were approved by the Animal Care and Use Committee of RIKEN Kobe Branch (MAH21-10).

PET Scans

PET scans in conscious marmosets were performed with a PET scanner (microPET Focus220; Siemens Medical Solutions, Knoxville, TN) as previously described (Yokoyama et al., 2010). After cannulation via a tail vein, animals were fixed in a sitting position (tilted to 45°) in the scanner. For PET scans in anesthetized animals, inhalation induction with sevoflurane and then isoflurane anesthesia was maintained at 1% concentration, with monitoring of heart rate (150–200 beats/min) and peripheral oxygen saturation (>98%) with pulse oximetry (BSM-3592; Nihon Kohden, Tokyo, Japan). Animals were laid in the face-up position on a bed with the heads softly fixed by round ended ear bars and placed horizontally in the PET scanner. For both conscious and anesthetized animals, a transmission scan with a ^{68}Ge-^{68}Ga pin source was performed for 30 min before an emission scan.

We used 2 kinds of PET probes: ^{18}F-F13714 and ^{18}F-MPPF (Figure 1). According to a previous method (Lemoine et al., 2012), ^{18}F-F13714 was prepared by aromatic nucleophilic substitution reaction of the previously reported nitro precursor (3 mg, 6.7 μmol) with ^{18}F-KF/Kryptofix 2.2.2 in DMSO (200 μL). ^{18}F-Fluoride anion was produced by a cyclotron (HM-12S; Sumitomo Heavy Industry Ltd., Tokyo, Japan). The radiochemical purity and chemical purity were >99% and >93%, respectively. The specific activity was 67.7 ± 13.4 GBq/μmol at the end of synthesis. According to a previous method (Le Bars et al., 1998), ^{18}F-MPPF was prepared by aromatic nucleophilic substitution reaction of the previously reported nitro precursor (5 mg, 10.8 μmol) with ^{18}F-KF/Kryptofix 2.2.2 in DMSO (500 μL). The radiochemical purity and chemical purity were both >99%. The specific activity was 182.5 ± 65.6 GBq/μmol at the end of synthesis. In both tracers, PET scans were performed for 90 minutes immediately after bolus injection of radiolabeled tracers (^{18}F-F13714: 162.2 ± 21.4 MBq/kg; ^{18}F-MPPF: 158.6 ± 14.4 MBq/kg). Images were acquired with a 3-dimensional list-mode and reconstructed by a filtered back projection algorithm using a Hanning filter cut-off 0.5 cycles/pixels with the attenuation correction using blank and transmission images. A spatial resolution at the center of the field of view is approximately 1.35 mm in full width at half-maximum. The dynamic histogram acquired during 90 minutes (6 × 10 seconds, 6 × 30 seconds, 11 × 60 seconds, 15 × 180 seconds, 3 × 600 seconds) was used for data analyses.

Data Analysis

Reconstructed images were processed with image analysis software PMOD (version 3.5, PMOD Technologies Ltd., Zurich, Switzerland). First, individual PET images were aligned on each individual MR image by rigid matching using PMOD's image registration and fusion tool (PFUS). Next, the template of the brain MR image that was previously prepared (Yokoyama et al., 2013) was used for normalization of individual PET images. PET images of the brain were deskulled according to the structural information from individual brain MR images. Individual brain MR images were then registered to the standard space of the template brain MR image by brain normalization. By using these registration matrices, PET images were transformed and normalized.

The normalized individual PET images were used to elucidate the quantitative ^{18}F-F13714 and ^{18}F-MPPF binding to 5-HT$_{1A}$ receptors in the brain. We calculated binding potential (BP_{ND}) by quantifying the ratio at equilibrium of specifically bound radioligand to that of nondisplaceable radioligand in brain tissue using a nonlinear fitting method involving a simplified reference tissue model (SRTM), using cerebellum as a reference region and the cingulate cortex for ^{18}F-F13714 or in the hippocampus for ^{18}F-MPPF as a high expression region. Though in vitro autoradiography studies showed that ^{18}F-F13714 and ^{18}F-MPPF have almost no specific binding in cerebellum (Le Bars et al., 1998; Lemoine et al., 2012), there is controversy as to whether the cerebellum is devoid of the 5HT$_{1A}$ receptors in vivo (Parsey et al., 2010; Shrestha et al., 2012). However, we have confirmed in this study that the time activity curves of ^{18}F-F13714 and ^{18}F-MPPF in the cerebellum show the lowest uptake among brain regions, and also that when the ROI of cerebellum is divided into the gray and white matter, the shape of these TACs are very similar to each other. Therefore, using cerebellum as a reference region should be meaningful in our PET study at present. The parametric images of BP_{ND} were created by SRTM2 with fixing of k2' estimated by SRTM. Regional BP_{ND} values were obtained by applying several anatomical regions of interest (ROIs) that were drawn manually in the template brain MR image with reference to the stereotaxic brain atlas of the common marmoset (Paxinos et al., 2011) (Figure 5) on the following regions: the frontal cortex, parietal cortex, temporal cortex, occipital cortex, cingulate cortex,

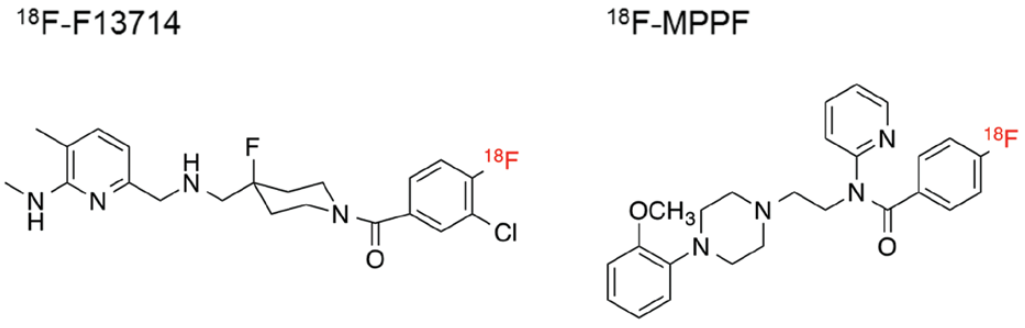

Figure 1. Chemical structures of ^{18}F-F13714 and ^{18}F-MPPF.

insular cortex, caudate nucleus, putamen, amygdale, hippocampus, hypothalamus, thalamus, raphe, and tectum (Figure 5). Volumes of interest consisted of ROIs of 299.1 mm^3 on average, with 811.3 mm^3 at maximum in the temporal cortex and 1.3 mm^3 at minimum in the raphe.

The between-subject variability of BP_{ND} in each region was assessed for both conditions as the CV as follows:

$$CV = \frac{SD}{Mean} \times 100\ \%$$

The within-subject variability across conditions was assessed for each region as follows:

$$VAR = \frac{|conscious - anesthesia|}{(conscious + anesthesia)/2} \times 100\%$$

The reliability of the measurement per region was evaluated by comparing the within-subject variability (WS) to the between-subject variability (BS) in terms of intraclass correlation coefficient ICC (1,1) as follows, where the MSS represents mean sum of squares and is calculated for the WS and the BS situation:

$$ICC = \frac{BSMSS - WSMSS}{BSMSS + WSMSS}$$

Statistics

The effect of isoflurane on regional BP_{ND} was analyzed separately by 2-way ANOVA (region × condition) for ^{18}F-F13714 and ^{18}F-MPPF. Differences in BP_{ND} between conscious and anesthesia scans were tested using a paired *t* test in each ROI. The comparison regression between ^{18}F-F13714 and ^{18}F-MPPF across ROIs used the Deming regression model, taking measurement errors for both parameters separately on conscious and anesthetic scans. Statistical analyses were performed using R2.8.1, and a *P* value of .05 was defined as the threshold of statistical significance.

RESULTS

PET Scans with ^{18}F-F13714

^{18}F-F13714 uptake in the marmoset brain was rapid and showed apparently quasi-irreversible kinetics over the observation period (Figure 2), suggesting very high affinity binding of this tracer to the 5-HT_{1A} receptor or, potentially, a rapid internalization of the receptors, although this remains speculative. In conscious animals, the distributed radioactivity indicated a distinctive pattern with a high level of uptake in the cingulate and insular cortices, raphe nucleus, thalamus, and tectum. Intermediate uptake was observed in the hippocampus, other cortical areas, amygdala, and hypothalamus, but also in the caudate and putamen. Low uptake was observed in the cerebellum (Figure 2a).

In animals anesthetized with isoflurane, there were subtle changes in the shape of the time activity curves, with an initial rapid rise followed by a slight decrease before showing uptake levels and quasi-irreversible kinetics similar to those observed in conscious animals (Figure 2b). There were differences in the uptake level in the various brain regions in anesthetized animals compared with conscious animals, with higher uptake in the hippocampus, amygdala, and hypothalamus and lower uptake in the caudate nucleus and putamen (see below for statistical information).

Variability was observed in ^{18}F-F13714 binding between individual animals in both conscious and anesthetic conditions (Table 1). Regional BP_{ND} values had a moderate variation across subjects in conscious animals (CV: 26.1–58.0%, average 38.4%), but a higher variability in anesthetized animals (CV: 17.4–103.6%, average 53.7%). Two-way ANOVA revealed that isoflurane did not significantly change overall ^{18}F-F13714 BP_{ND} ($F(1, 42) = 0.0013$, $P = .971$), as the effects of anesthesia were region specific and not unidirectional. A significant interaction effect of region and condition was observed ($F(13, 42) = 4.392$, $P = .0001$). Tukey's posthoc comparison after Bonferroni correction showed that isoflurane significantly increased ^{18}F-F13714 BP_{ND} in the hippocampus ($t = 3.65$, $P < .01$) and hypothalamus ($t = 3.19$, $P < .05$) and decreased in the putamen ($t = 3.19$, $P < .05$). The high ICC (0.37–0.95, average 0.73) indicated a good reliability of individual variations in regional ^{18}F-F13714 binding, even across conscious and anesthetic conditions.

PET Scans with ^{18}F-MPPF

^{18}F-MPPF uptake was similar in shape of the time activity curves between the conscious and anesthetic conditions, with a rapid rise and gradual decline, although the uptake level and variance was generally increased in anesthetized animals (Figure 3). A high level of uptake was observed in the hippocampus and amygdala; moderate uptake in the cingulate, insular, and frontal cortices, raphe nucleus, and tectum; lower uptake in the thalamus, striatum, hypothalamus, and other cortical areas; and low uptake in the cerebellum. There was some variation between individual animals in ^{18}F-MPPF regional BP_{ND} values (although this was lower than that observed with ^{18}F-F13714): under conscious conditions, CV values were 9.4% to 48.4%, average 22.5%; under anesthetized conditions: CV values were 10.1% to 94.5%, average 36.5% (Table 2).

Two-way ANOVA revealed that isoflurane significantly increased ^{18}F-MPPF BP_{ND} ($F(1, 42) = 10.03$, $P = .0029$), while there was no statistically significant interaction effect for individual brain regions ($F(13, 42) = 0.56$ $P = .87$). Tukey's posthoc comparison after Bonferroni correction indicated no significant effect of isoflurane on ^{18}F-MPPF BP_{ND} in any ROIs. The very low ICC (average 0.04), except for the amygdala (0.93), suggests that the individual variation of regional ^{18}F-MPPF binding was inconsistent between conscious and anesthetic conditions.

Comparison of ^{18}F-F13714 and ^{18}F-MPPF Binding Distribution

There were notable differences in BP_{ND} between ^{18}F-F13714 and ^{18}F-MPPF across the ROIs (Figure 4). ^{18}F-MPPF showed a markedly higher contrast than ^{18}F-F13714, especially in the binding-rich regions, with an approximately 3 times higher BP_{ND}. Thus maximal BP_{ND} for ^{18}F-MPPF amounted to 1.5 to 2.0 in the hippocampus and amygdala, whereas maximal BP_{ND} for ^{18}F-F13714 amounted to about 0.5 in the insular cortex and raphe nucleus. Other brain regions did not show marked differences in BP_{ND} between PET probes: both ^{18}F-F13714 and ^{18}F-MPPF yielded BP_{ND} values of about 0.2 to 0.3 in the caudate nucleus, putamen, and thalamus (Figure 4).

Averaged BP_{ND} images from all subjects for ^{18}F-F13714 and ^{18}F-MPPF are shown in Figure 5. Notably, there was no correlation of BP_{ND} between the 2 tracers in conscious animals ($F(1,12) = 1.19$, $P = .30$), while a significant correlation was observed under isoflurane anesthesia ($F(1,12) = 8.92$, $P = .01$) (Figure 6). These results suggest that the population of 5-HT_{1A} receptors identified by ^{18}F-F13714 was proportional to that identified by ^{18}F-MPPF under anesthesia conditions, but not when PET experiments were carried out in conscious marmosets.

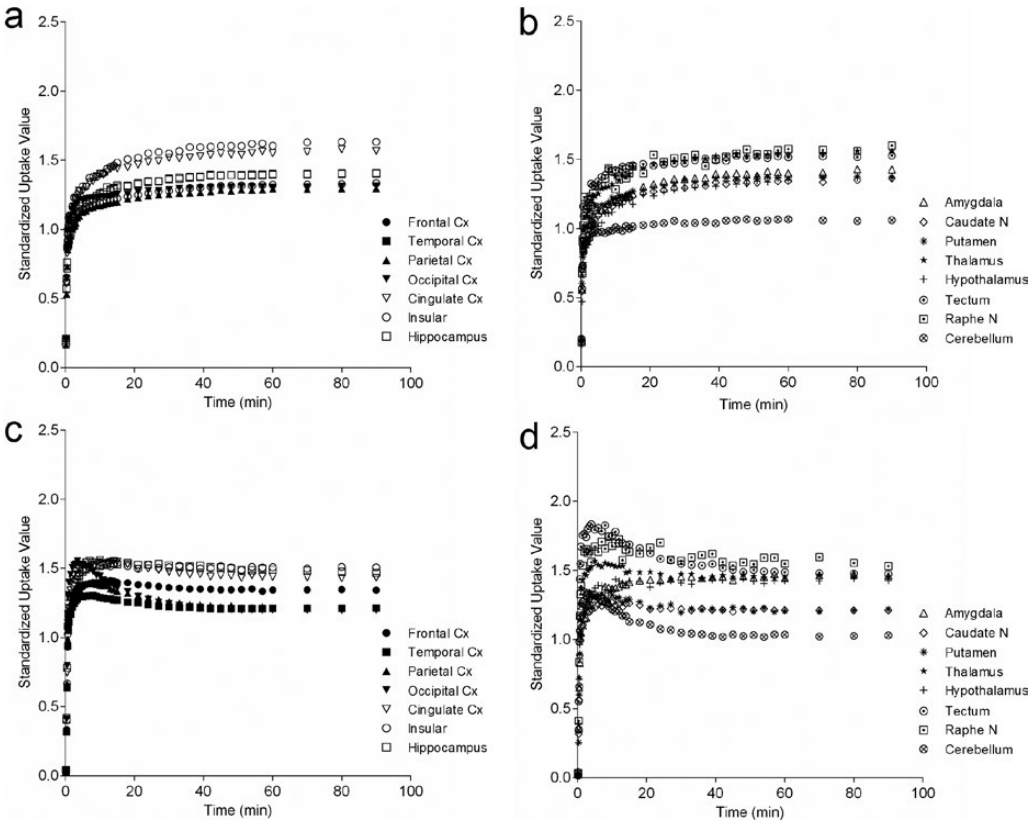

Figure 2. Time activity curves of ^{18}F-F13714 uptake in cortical (a and c) and subcortical (b and d) regions of interest in conscious (a-b) and isoflurane anesthetized (c-d) conditions. Anatomical locations of regions of interest refer to Figure 5. Data are mean values (n=4) to allow easy viewing, but relatively higher variability is found in each point of value in conscious (a-b) than in isoflurane anesthetized (c-d) conditions.

Table 1. Regional ^{18}F-F13714 BP_{ND} Across Individuals under Conscious and Isoflurane Anesthesia Conditions

	Conscious		Isoflurane				
Regions	**BP_{ND} (mean±SD)**	**CV (%)**	**BP_{ND} (mean±SD)**	**CV (%)**	**VAR (%, mean±SD)**	**ICC**	**Paired *t***
Frontal Cx	0.32±0.13	40.8	0.32±0.18	56.6	17.4±10.0	0.92	0.021
Temporal Cx	0.26±0.08	32.5	0.18±0.14	73.4	48.3±41.1	0.63	1.900
Parietal Cx	0.21±0.12	58.0	0.20±0.14	70.8	24.7±22.7	0.93	0.286
Occipital Cx	0.23±0.11	49.0	0.18±0.14	77.2	54.5±60.8	0.81	1.339
Cingulate Cx	0.46±0.15	32.5	0.42±0.20	48.3	17.2±18.4	0.89	1.141
Insular	0.53±0.16	30.3	0.47±0.21	45.0	16.0±22.1	0.84	1.480
Hippocampus	0.32±0.16	50.5	0.47±0.17	37.2	40.6±23.1	0.62	3.653*
Amygdala	0.33±0.15	44.4	0.44±0.21	47.6	27.2±16.6	0.76	2.660
Caudate N	0.27±0.11	42.3	0.19±0.17	89.5	55.2±46.8	0.78	1.935
Putamen	0.29±0.07	26.1	0.16±0.16	103.6	93.4±82.6	0.37	3.186*
Thalamus	0.45±0.14	31.3	0.42±0.14	33.9	15.2±12.6	0.88	0.778
Hypothalamus	0.28±0.14	49.9	0.40±0.11	26.4	42.8±32.1	0.41	3.193*
Tectum	0.44±0.13	29.3	0.47±0.12	24.6	14.0±11.8	0.83	0.907
Raphe N	0.47±0.10	20.8	0.52±0.09	17.4	17.7±11.1	0.51	1.477
Mean		38.4		53.7		0.73	

Discussion

This is the first report on PET imaging of ^{18}F-F13714, a novel, selective 5-HT_{1A} receptor agonist PET probe, in nonhuman primate brain. The results indicate that it displays a highly distinctive brain distribution pattern in conscious and anesthetized common marmosets that differs markedly from that of a well-characterized antagonist PET probe, ^{18}F-MPPF.

The overall brain distribution pattern of ^{18}F-F13714 binding in marmosets exhibited some consistency with previous reports of 5-HT_{1A} receptor densities in rats, baboons, rhesus monkeys, and humans determined with other PET probes, including ^{18}F-MPPF (Pike et al., 1996; Maeda et al., 2001; Costes et al., 2007; Milak et al., 2010, 2011; Wooten et al., 2011). Thus, higher binding of ^{18}F-F13714 was observed in regions classically associated with 5-HT_{1A} receptor expression, including the cortical regions, hippocampus, amygdala, hypothalamus, and raphe nucleus (Figures 4 and 5). However, the intensity of the binding distribution in these brain regions was strikingly different from that seen with ^{18}F-MPPF. Indeed, ^{18}F-F13714 showed lower binding in the

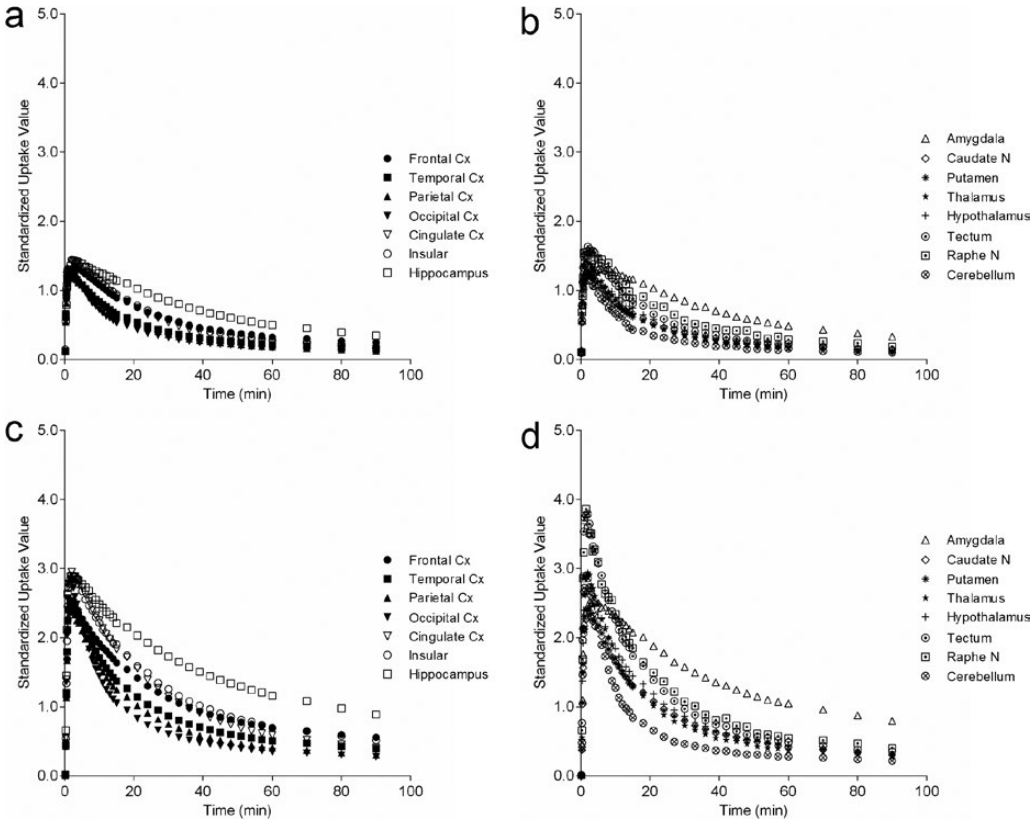

Figure 3. Time activity curves of ^{18}F-MPPF uptake in cortical (a and c) and subcortical (b and d) regions of interest in conscious (a-b) and isoflurane-anesthetized (c-d) conditions. Anatomical locations of regions of interest (ROIs) refer to Figure 5. Data are mean values (n = 4) to allow easy viewing, but there is similar variability in each point of value in conscious (a-b) than in isoflurane-anesthetized (c-d) conditions.

Table 2. Regional ^{18}F-MPPF BP_{ND} across Individuals under Conscious and Isoflurane Anesthesia Conditions

	Conscious		Isoflurane				
Regions	BP_{ND} (mean ± SD)	CV (%)	BP_{ND} (mean ± SD)	CV (%)	VAR (%, mean ± SD)	ICC	Paired t
Frontal Cx	0.89 ± 0.21	23.6	0.94 ± 0.33	35.3	30.6 ± 23.7	-0.54	0.385
Temporal Cx	0.39 ± 0.04	9.4	0.53 ± 0.15	28.9	30.8 ± 18.0	-0.12	1.107
Parietal Cx	0.28 ± 0.02	8.0	0.33 ± 0.23	68.0	58.7 ± 45.0	0.07	0.387
Occipital Cx	0.26 ± 0.12	48.4	0.20 ± 0.17	87.2	92.0 ± 65.9	-0.72	0.462
Cingulate Cx	0.76 ± 0.07	9.8	0.93 ± 0.17	18.8	25.3 ± 14.0	-0.54	1.335
Insular	0.89 ± 0.14	15.3	1.09 ± 0.37	34.2	23.8 ± 20.2	0.10	1.590
Hippocampus	1.66 ± 0.19	11.6	1.98 ± 0.20	10.1	18.0 ± 7.3	0.03	2.593
Amygdala	1.57 ± 0.28	18.0	1.64 ± 0.24	14.6	5.4 ± 3.7	0.93	0.539
Caudate N	0.35 ± 0.10	28.0	0.38 ± 0.12	30.7	25.0 ± 19.0	0.16	0.227
Putamen	0.28 ± 0.15	52.0	0.40 ± 0.38	94.5	45.6 ± 39.5	0.21	0.966
Thalamus	0.28 ± 0.09	31.1	0.36 ± 0.06	17.4	27.8 ± 16.6	0.39	0.643
Hypothalamus	0.39 ± 0.05	13.0	0.51 ± 0.12	22.8	25.5 ± 21.9	-0.30	0.962
Tectum	0.65 ± 0.15	23.8	0.82 ± 0.17	20.2	24.1 ± 13.1	0.35	1.382
Raphe N	0.92±0.21	22.4	0.94±0.25	26.3	21.2±8.7	0.56	0.193
Mean		22.5		36.3		0.04	

hippocampus and amygdala than in cingulate and insular cortices, particularly in conscious marmosets. This is reminiscent of the preferential binding in cortical areas previously reported in cats using ^{18}F-F13714 and another agonist PET probe, ^{18}F-F15599 (Lemoine et al., 2010, 2012). In contrast, the antagonist tracer, ^{18}F-MPPF showed almost 2-fold higher binding to the hippocampus and amygdala compared with the cingulate and insular cortices, consistent with previous reports in rats, cats, and humans (Plenevaux et al., 2000; Passchier et al., 2001; Aznavour et al., 2006; Costes et al., 2007; Sibon et al., 2008). For ^{18}F-F13714, BP_{ND} value in the raphe nucleus was similar to that in the hippocampus; in contrast, the BP_{ND} value in the raphe nucleus for ^{18}F-MPPF was only one-half of that in the hippocampus (Figure 4). Further, ^{18}F-F13714 exhibited pronounced binding to the thalamus and hypothalamus, whereas these brain regions were only modestly labeled by ^{18}F-MPPF. Finally, ^{18}F-F13714 exhibited a noticeable labelling of the caudate nucleus and putamen, approaching that observed in the frontal cortex. In contrast, binding of ^{18}F-MPPF in the caudate and putamen amounted to less than one-half of that seen in the frontal cortex.

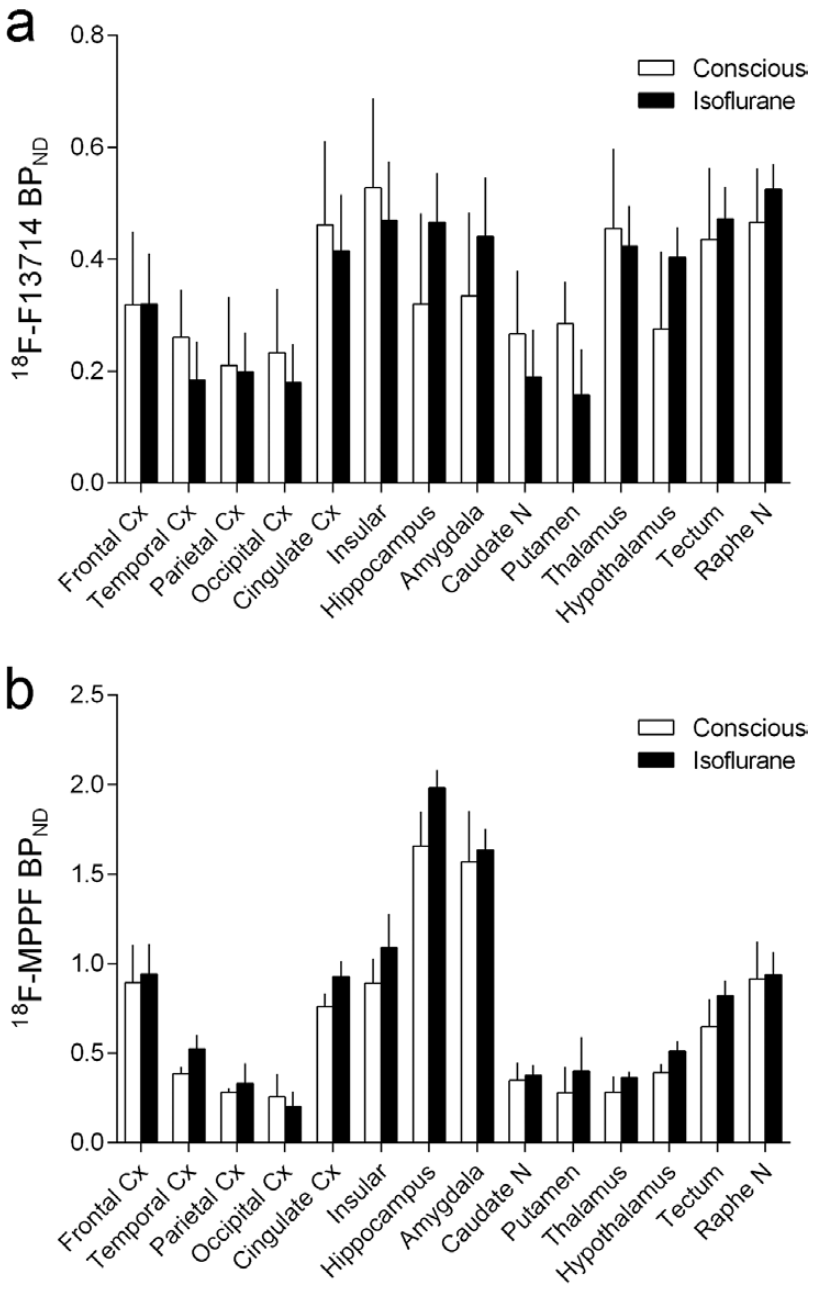

Figure 4. Serotonin (5-HT)1A receptor binding potential values with ^{18}F-F13714 (a) and ^{18}F-MPPF (b) in conscious (open column) and isoflurane anesthetized (filled column) conditions. Anatomical locations of regions of interest (ROIs) refer to Figure 4. Data are mean ± SD (n=4).

As discussed previously (Lemoine et al., 2012), F13714 is highly selective for 5-HT$_{1A}$ receptors, and its neurochemical and behavioral effects are blocked by a 5-HT$_{1A}$ receptor antagonist (WAY100635) (Assié et al., 2006; Iderberg et al., 2015). Accordingly, the in vitro autoradiographic labeling seen with ^{18}F-F13714 on rat brain sections was completely blocked by co-incubation with WAY-100635, and in vivo cat brain PET labelling was prevented by preinjection of WAY-100635 (Lemoine et al., 2012). These considerations suggest that differences in labeling patterns between the 2 tracers may relate to the agonist properties of ^{18}F-F13714 that enable it to distinguish a 5-HT$_{1A}$ receptor subpopulation of high-affinity sites (Assié et al., 2006; Maurel et al., 2007; Lemoine et al., 2012), a concept described previously for the 5-HT$_{1A}$ receptor in baboons with ^{11}C-CUMI-101 (agonist) and ^{11}C-WAY100635 (antagonist) (Kumar et al., 2012). In the case of F13714, extensive evidence supports the notion that it acts as a biased agonist that preferentially targets 5-HT$_{1A}$ receptors in specific brain regions, including the raphe, striatum, and thalamus (Assié et al., 2006; Iderberg et al., 2015; Becker et al., 2016).

Thus, F13714 potently inhibits 5-HT release in cortex and striatum (Assié et al., 2006; Iderberg et al., 2015), reverses L-DOPA-induced dyskinesia in Parkinsonian rats, and stimulates a BOLD signal in the raphe, striatum, and motor cortex (Becker et al., 2016), results that are consistent with the present study showing accentuated binding to these brain regions in marmoset brain. Although the molecular basis for this remains to be clarified, it is likely due to a preferential interaction of ^{18}F-F13714 with 5-HT$_{1A}$ receptors that are coupled to specific G-protein subtypes

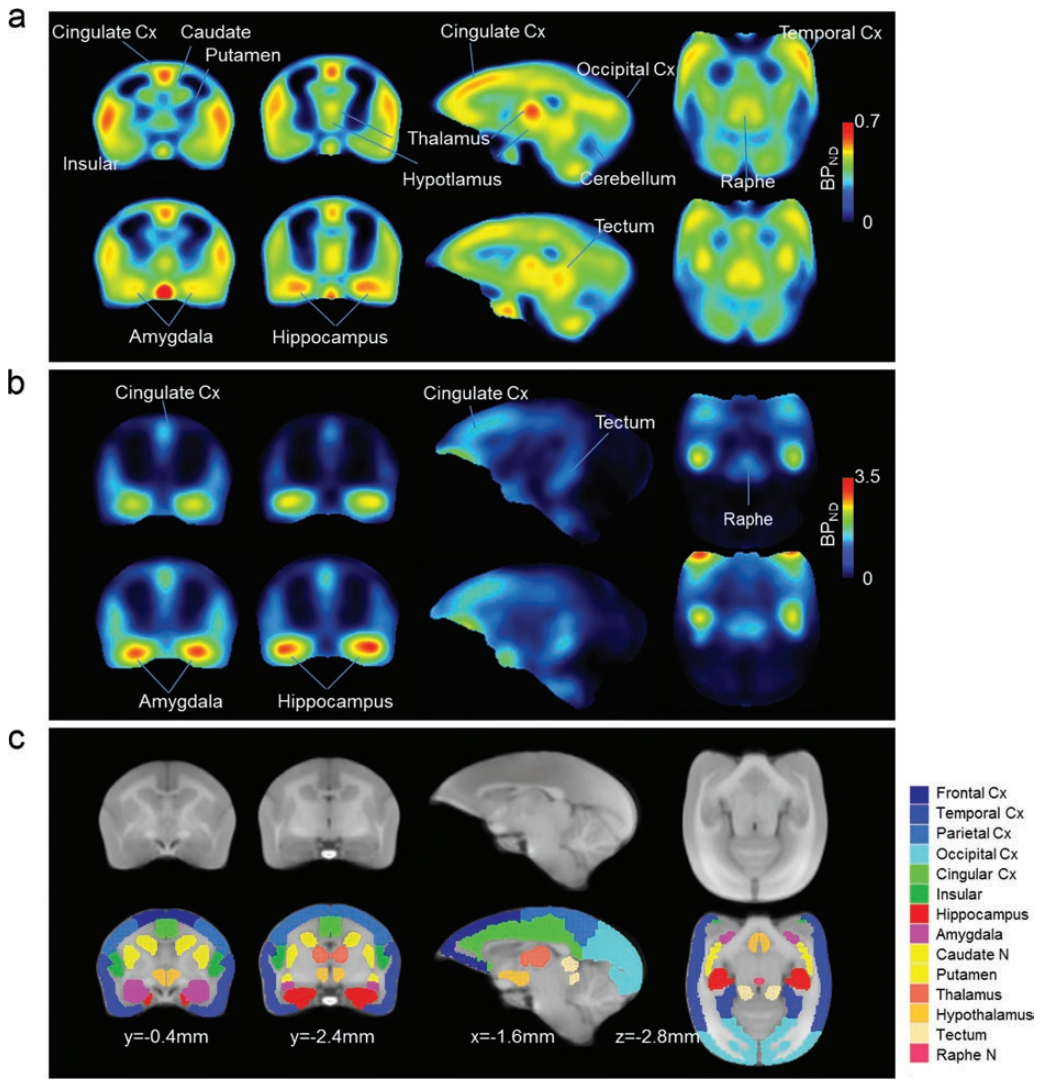

Figure 5. Serotonin (5-HT)1A receptor binding potential (BP_{ND}) images with ^{18}F-F13714 (a) and ^{18}F-MPPF (b) in conscious (top) and isoflurane (bottom) conditions. Note that the pseudo-color BP_{ND} scales differ between the 2 radiotracers: 0 to 0.7 for ^{18}F-F13714: 0 to 3.5 for ^{18}F-MPPF. MRI images corresponding to the anatomical regions shown in the positron emission tomography (PET) images are shown in (c). Names of separately colored areas on the lowermost MRI images are listed on the right, which represent regions of interest (ROIs) for evaluating BP_{ND} values in Tables 1 and 2 and in Figures 2 to 4. Numerical representations as x, y, z are the coordinates for the anterior commissure on the ac-pc line in the standard marmoset MRI prepared in our laboratory.

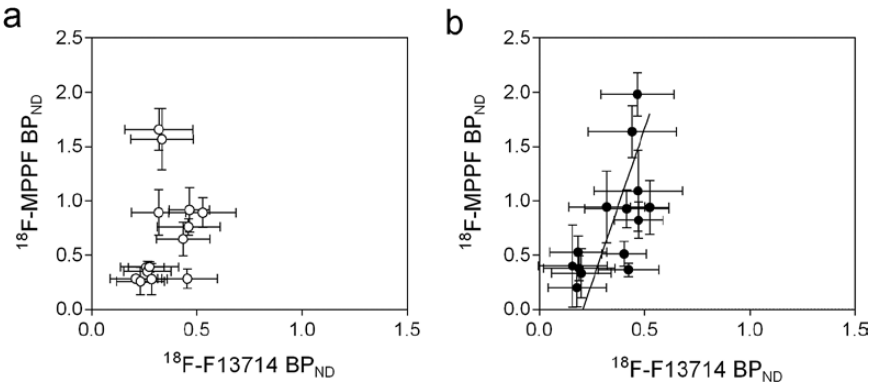

Figure 6. Correlation of Serotonin (5-HT)1A receptor binding potential values with an agonist tracer ^{18}F-F13714 and an antagonist tracer ^{18}F-MPPF in conscious (open circle) (a) and isoflurane-anesthetized (filled circle) conditions (b). Data are mean ± SD (n = 4).

and/or intracellular signaling mechanisms (Newman-Tancredi, 2011). The locus of these effects remains under investigation, but a potent activation of somatodendritic 5-HT_{1A} autoreceptors appears important. The present PET data clearly indicate that ^{18}F-F13714 binds to sites in the raphe (Figures 2, 4, and 5). Microdialysis studies show that F13714 potently inhibits 5-HT

release in both hippocampus and striatum (Assié et al., 2006; Iderberg et al., 2015), responses controlled by somatodendritic 5 HT_{1A} receptors. An ex vivo immediate early gene expression study showed that F13714 potently elicits increases in c-fos expression in dorsal and median raphe (Cussac et al., 2007). Taken together, these observations suggest that ^{18}F-F13714 has an accentuated activity at presynaptic 5-HT_{1A} receptors. However, it should be noted that, although binding profile of F13714 has been extensively characterized in the rat, in the marmoset brain it is still under investigation. Some caution is therefore warranted until further studies of this issue have been carried out.

Some additional points should be noted. Firstly, although the agonistic profile of ^{18}F-F13714 has not been directly demonstrated in marmoset brain, it may be inferred by the distinctive binding kinetics we observed in anesthetized animals. Indeed, whereas isoflurane caused a global increase in ^{18}F-MPPF uptake throughout the brain (Figure 3), binding kinetics of ^{18}F-F13714 showed region-specific changes. The binding in tectum and occipital cortex increased rapidly, peaked, and then decreased slightly before stabilizing. In contrast, binding in amygdala and frontal cortex did not show this temporal profile and resembled that observed in conscious marmosets (Figure 2). It is tempting to speculate that these different profiles may be caused by changes in endogenous serotonin levels, which, by competing for binding to 5-HT_{1A} receptors, could change the binding potential of ^{18}F-F13714. Indeed, isoflurane was reported to decrease extracellular 5-HT in the hippocampus and the frontal cortex (Whittington and Virág, 2006; Mukaida et al., 2007) and inhibit 5-HT neuron firing in the medullary raphe (Johansen et al., 2015). It may therefore be surmised that, because its agonist activity, ^{18}F-F13714 may have a higher sensitivity than for ^{18}F-MPPF for measuring receptor occupancy by endogenous synaptic 5-HT release.

The assertion that agonist PET probes can identify a subset of 5-HT_{1A} receptors whereas antagonist tracers label the total receptor population (Aznavour et al., 2006; Lemoine et al., 2010; Kumar et al., 2012; Billard et al., 2014) is supported by the observation that ^{18}F-F13714 showed lower BP_{ND} values than ^{18}F-MPPF in all brain regions. Linear regression of the binding potential values of 2 tracers in anesthetized marmosets achieved statistical significance (see Figure 6 and Results) and suggested that 5-HT_{1A} receptors labelled by ^{18}F-F13714 constitute about one-third of the total receptor population (Figure 6). This implies a ratio of approximately 1:2 for G-protein-coupled receptors in a high-affinity state to those in a low-affinity state. This ratio is similar to that reported using ^{11}C-CUMI-101 and ^{11}C-WAY100635 in anesthetized baboons, although the agonist activity of ^{11}C-CUMI-101 may be questionable (Hendry et al., 2011; Kumar et al., 2012; Shrestha et al., 2014). By contrast, there was no correlation in binding potential values between the 2 PET probes in conscious animals, possibly reflecting changes in extracellular 5-HT levels due to vigilance state. Indeed, consciousness affects serotonergic neurotransmission in forebrain structures including the hippocampus and hypothalamus (Portas et al., 1998; Park et al., 1999; Shouse et al., 2000; Python et al., 2001). Given that human PET studies are normally performed without an anesthetic, these results strengthen the rationale for testing both agonist and antagonist PET probes when quantifying 5-HT_{1A} receptor function.

It is surmised that agonist PET probes such as ^{18}F-F13714 may be more suitable than ^{18}F-MPPF for detecting changes in 5-HT_{1A} receptor function elicited by therapeutic agents such as antidepressants or antipsychotics, many of which act as agonists at this target (see Introduction). Agonist PET probes would also be desirable when assessing the association between 5-HT_{1A} receptors and behavioral phenotypes. The involvement of the 5-HT_{1A} receptor in various aspects of cognition, depression, and anxiety has been amply demonstrated (Harder and Ridley, 2000; Gingrich and Hen, 2001; Albert et al., 2014; Stiedl et al., 2015), but a human database of 5-HT_{1A} receptor binding by PET with an antagonist probe ^{11}C-WAY100635 showed high between-subject variability and failed to find any correlations with personality variables (Rabiner et al., 2002), while several studies reported an association with anxious or aggressive traits in smaller sample sizes (Tauscher et al., 2001; Parsey et al., 2002).

Some limitations of the present study should be mentioned. Firstly, the data herein are based on a small cohort of marmosets (4 animals). Nevertheless, using the same animals in all conditions allowed us to show clear differences between the 5-HT agonist and antagonist and between conscious and isoflurane conditions. Secondly, there are no data directly showing the selectivity and agonist behavior of ^{18}F-F13714 binding for 5-HT_{1A} receptors in the marmoset brain, although the selectivity of F13714 has been documented in vitro (Assié et al., 2006). Thirdly, the existence of 2 distinct affinity states of 5-HT_{1A} receptors (high affinity, "functional" state and lower affinity, nonfunctional state) have not yet been directly demonstrated in vivo and therefore warrants further evaluation (Cumming et al., 2002; Skinbjerg et al., 2012).

Conclusions

We successfully evaluated 5-HT_{1A} receptor binding distribution in the marmoset brain using a novel biased agonist PET probe, ^{18}F-F13714, in comparison with a well-characterized antagonist PET probe, ^{18}F-MPPF. There were striking differences in the pattern of binding between the 2 PET probes. Whereas ^{18}F-MPPF showed highest binding in hippocampus and amygdala, ^{18}F-F13714 showed highest labeling in other regions, including insular and cingulate cortex, thalamus, and raphe nucleus. Marked binding was noted in caudate nucleus and putamen. This distinctive pattern of labeling correlates with results from phMRI brain imaging (Becker et al., 2016) and underpin the remarkably potent antidyskinetic activity of F13714 in rat models of Parkinson's disease (Iderberg et al., 2015).

The present study also found marked individual- and region-specific differences under isoflurane-anesthetized vs conscious conditions of PET imaging. Notably, ^{18}F-F13714 showed a marked difference to ^{18}F-MPPF with respect to susceptibility to isoflurane, suggesting that the functional state of 5-HT_{1A} receptors is strongly influenced by anesthesia.

Taken together, these findings highlight the importance of investigating the brain imaging of 5-HT_{1A} receptors using agonist PET probes, such as ^{18}F-F13714, and suggest that caution is necessary when interpreting results on serotonin receptor PET imaging when using anesthetized animals. Further studies are required to extend the present observations to human: if biased agonist activity at 5-HT_{1A} receptors can also be observed under clinical conditions, new opportunities may emerge for treatment of neuropsychiatric and neurological disorders involving serotonergic systems.

Acknowledgments

We thank Dr T. Hayashi and Dr Y. Wada for their assistance in performing animal MRI and PET and Mr T. Ose and Ms E. Hayashinaka for technical assistance.

This work was supported in part by a grant of the Bilateral Joint Research Project from Japan Society for the Promotion of Science (JSPS), Japanese Government (to H.O.), JSPS KAKENHI 25293254 and 26118517 (to C.Y.), and the program for Brain Mapping by Integrated Neurotechnologies for Disease Studies (Brain/MINDS) from Japan Agency for Medical Research and Development.

Statement of Interest

A.N.-T. is an employee and stock-holder of Neurolixis Inc. In the last 3 years he has received consulting honoraria from Lundbeck, Adamed, and Theranexus.

References

Albert PR, Vahid-Ansari F, Luckhart C (2014) Serotonin-prefrontal cortical circuitry in anxiety and depression phenotypes: pivotal role of pre- and post-synaptic 5-HT1A receptor expression. Front Behav Neurosci 8:199.

Assié M-B, Lomenech H, Ravailhe V, Faucillon V, Newman-Tancredi A (2006) Rapid desensitization of somatodendritic 5-HT1A receptors by chronic administration of the high-efficacy 5-HT1A agonist, F13714: a microdialysis study in the rat. Br J Pharmacol 149:170–178.

Aznavour N, Rbah L, Léger L, Buda C, Sastre J- P, Imhof A, Charnay Y, Zimmer L (2006) A comparison of in vivo and in vitro neuroimaging of 5-HT 1A receptor binding sites in the cat brain. J Chem Neuroanat 31:226–232.

Aznavour N, Zimmer L (2007) [^{18}F]MPPF as a tool for the in vivo imaging of 5-HT1A receptors in animal and human brain. Neuropharmacology 52:695–707.

Bantick RA, Montgomery AJ, Bench CJ, Choudhry T, Malek N, McKenna PJ, Quested DJ, Deakin JFW, Grasby PM (2004a) A positron emission tomography study of the 5-HT1A receptor in schizophrenia and during clozapine treatment. J Psychopharmacol (Oxf) 18:346–354.

Bantick RA, Rabiner EA, Hirani E, de Vries MH, Hume SP, Grasby PM (2004b) Occupancy of agonist drugs at the 5-HT1A receptor. Neuropsychopharmacol Off Publ Am Coll Neuropsychopharmacol 29:847–859.

Becker G, Bolbos R, Costes N, Redoute J, Newman-Tancredi A, Zimmer L (2016) Selective serotonin 5-HT1A receptor biased agonists elicit distinct brain activation patterns: a pharmacoMRI study. Sci Rep 6:26633.

Billard T, Le Bars D, Zimmer L (2014) PET radiotracers for molecular imaging of serotonin 5-HT1A receptors. Curr Med Chem 21:70–81.

Celada P, Bortolozzi A, Artigas F (2013) Serotonin 5-HT1A receptors as targets for agents to treat psychiatric disorders: rationale and current status of research. CNS Drugs 27:703–716.

Costes N, Zimmer L, Reilhac A, Lavenne F, Ryvlin P, Le Bars D (2007) Test-retest reproducibility of ^{18}F-MPPF PET in healthy humans: a reliability study. J Nucl Med 48:1279–1288.

Cumming P, Wong DF, Gillings N, Hilton J, Scheffel U, Gjedde A (2002) Specific binding of [(11)C]raclopride and N-[(3)H]propyl-norapomorphine to dopamine receptors in living mouse striatum: occupancy by endogenous dopamine and guanosine triphosphate-free G protein. J Cereb Blood Flow Metab 22:596–604.

Cussac D, Lauressergues E, Berrichon G, Sammut M, Newman-Tancredi A, Buritova Y (2007) F15599, a 5-HT$_{1A}$ agonist that preferentially targets post-synaptic receptors: 1) activity on ERK1/2 phosphorylation and c-fos induction. In: Abstract of Society for Neurosciences 170.7/EE10, San Diego.

de Boer SF, Newman-Tancredi A (2016) Anti-aggressive effects of the selective high-efficacy "biased" 5-HT$_{1A}$ receptor agonists F15599 and F13714 in male WTG rats. Psychopharmacology (Berl) 233:937–947.

Elfving B, Bjørnholm B, Knudsen GM (2003) Interference of anaesthetics with radioligand binding in neuroreceptor studies. Eur J Nucl Med Mol Imaging 30:912–915.

Fisher PM, Meltzer CC, Ziolko SK, Price JC, Moses-Kolko EL, Berga SL, Hariri AR (2006) Capacity for 5-HT$_{1A}$-mediated autoregulation predicts amygdala reactivity. Nat Neurosci 9:1362–1363.

Gingrich JA, Hen R (2001) Dissecting the role of the serotonin system in neuropsychiatric disorders using knockout mice. Psychopharmacology (Berl) 155:1–10.

Harder JA, Ridley RM (2000) The 5-HT$_{1A}$ antagonist, WAY 100 635, alleviates cognitive impairments induced by dizocilpine (MK-801) in monkeys. Neuropharmacology 39:547–552.

Hendry N, Christie I, Rabiner EA, Laruelle M, Watson J (2011) In vitro assessment of the agonist properties of the novel 5-HT$_{1A}$ receptor ligand, CUMI-101 (MMP), in rat brain tissue. Nucl Med Biol 38:273–277.

Iderberg H, McCreary AC, Varney MA, Cenci MA, Newman-Tancredi A (2015) Activity of serotonin 5-HT(1A) receptor "biased agonists" in rat models of Parkinson's disease and L-DOPA-induced dyskinesia. Neuropharmacology 93:52–67.

Johansen SL, Iceman KE, Iceman CR, Taylor BE, Harris MB (2015) Isoflurane causes concentration-dependent inhibition of medullary raphé 5-HT neurons in situ. Auton Neurosci Basic Clin 193:51–56.

Kiser D, Steemers B, Branchi I, Homberg JR (2012) The reciprocal interaction between serotonin and social behaviour. Neurosci Biobehav Rev 36:786–798.

Koek W, Vacher B, Cosi C, Assié MB, Patoiseau JF, Pauwels PJ, Colpaert FC (2001) 5-HT$_{1A}$ receptor activation and antidepressant-like effects: F 13714 has high efficacy and marked antidepressant potential. Eur J Pharmacol 420:103–112.

Kranz GS, Kasper S, Lanzenberger R (2010) Reward and the serotonergic system. Neuroscience 166:1023–1035.

Kumar JSD, Majo VJ, Hsiung S-C, Millak MS, Liu K-P, Tamir H, Prabhakaran J, Simpson NR, Van Heertum RL, Mann JJ, Parsey RV (2006) Synthesis and in vivo validation of [O-methyl-^{11}C]2-{4-[4-(7-methoxynaphthalen-1-yl)piperazin-1-yl]butyl}-4-methyl-2H-[1,2,4]triazine-3,5-dione: a novel 5-HT$_{1A}$ receptor agonist positron emission tomography ligand. J Med Chem 49:125–134.

Kumar JSD, Milak MS, Majo VJ, Prabhakaran J, Mali P, Savenkova L, Mann JJ, Parsey RV (2012) Comparison of high and low affinity serotonin 1A receptors by PET in vivo in nonhuman primates. J Pharmacol Sci 120:254–257.

Lancelot S, Zimmer L (2010) Small-animal positron emission tomography as a tool for neuropharmacology. Trends Pharmacol Sci 31:411–417.

Lanzenberger RR, Mitterhauser M, Spindelegger C, Wadsak W, Klein N, Mien L-K, Holik A, Attarbaschi T, Mossaheb N, Sacher J, Geiss-Granadia T, Kletter K, Kasper S, Tauscher J (2007) Reduced serotonin-1A receptor binding in social anxiety disorder. Biol Psychiatry 61:1081–1089.

Le Bars D, Lemaire C, Ginovart N, Plenevaux A, Aerts J, Brihaye C, Hassoun W, Leviel V, Mekhsian P, Weissmann D, Pujol JF, Luxen A, Comar D (1998) High-yield radiosynthesis and preliminary in vivo evaluation of p-[^{18}F]MPPF, a fluoro analog of WAY-100635. Nucl Med Biol 25:343–350.

Lemoine L, Verdurand M, Vacher B, Blanc E, Le Bars D, Newman-Tancredi A, Zimmer L (2010) [^{18}F]F15599, a novel 5-HT$_{1A}$ recep-

tor agonist, as a radioligand for PET neuroimaging. Eur J Nucl Med Mol Imaging 37:594–605.

Lemoine L, Becker G, Vacher B, Billard T, Lancelot S, Newman-Tancredi A, Zimmer L (2012) Radiosynthesis and preclinical evaluation of ^{18}F-F13714 as a fluorinated 5-HT$_{1A}$ receptor agonist radioligand for PET neuroimaging. J Nucl Med 53:969–976.

Li C-X, Patel S, Auerbach EJ, Zhang X (2013) Dose-dependent effect of isoflurane on regional cerebral blood flow in anesthetized macaque monkeys. Neurosci Lett 541:58–62.

Maeda J, Suhara T, Ogawa M, Okauchi T, Kawabe K, Zhang MR, Semba J, Suzuki K (2001) In vivo binding properties of [carbonyl-^{11}C]WAY-100635: effect of endogenous serotonin. Synapse 40:122–129.

Maurel JL, Autin J-M, Funes P, Newman-Tancredi A, Colpaert F, Vacher B (2007) High-efficacy 5-HT$_{1A}$ agonists for antidepressant treatment: a renewed opportunity. J Med Chem 50:5024–5033.

Milak MS, DeLorenzo C, Zanderigo F, Prabhakaran J, Kumar JSD, Majo VJ, Mann JJ, Parsey RV (2010) In vivo quantification of human serotonin 1A receptor using ^{11}C-CUMI-101, an agonist PET radiotracer. J Nucl Med 51:1892–1900.

Milak MS, Severance AJ, Prabhakaran J, Kumar JSD, Majo VJ, Ogden RT, Mann JJ, Parsey RV (2011) In vivo serotonin-sensitive binding of [^{11}C]CUMI-101: a serotonin 1A receptor agonist positron emission tomography radiotracer. J Cereb Blood Flow Metab 31:243–249.

Mukaida K, Shichino T, Koyanagi S, Himukashi S, Fukuda K (2007) Activity of the serotonergic system during isoflurane anesthesia. Anesth Analg 104:836–839.

Mukherjee J, Bajwa AK, Wooten DW, Hillmer AT, Pan M-L, Pandey SK, Saigal N, Christian BT (2016) Comparative assessment of (18) F-Mefway as a serotonin 5-HT$_{1A}$ receptor PET imaging agent across species: Rodents, nonhuman primates, and humans. J Comp Neurol 524:1457–1471.

Newman-Tancredi A (2011) Biased agonism at serotonin 5-HT$_{1A}$ receptors: preferential postsynaptic activity for improved therapy of CNS disorders. Neuropsychiatry 1:149–164.

Newman-Tancredi A, Martel J-C, Assié M-B, Buritova J, Lauressergues E, Cosi C, Heusler P, Bruins Slot L, Colpaert FC, Vacher B, Cussac D (2009) Signal transduction and functional selectivity of F15599, a preferential post-synaptic 5-HT$_{1A}$ receptor agonist. Br J Pharmacol 156:338–353.

Olivier B (2015) Serotonin: a never-ending story. Eur J Pharmacol 753:2–18.

Park SP, Lopez-Rodriguez F, Wilson CL, Maidment N, Matsumoto Y, Engel Jr. J (1999) In vivo microdialysis measures of extracellular serotonin in the rat hippocampus during sleep–wakefulness. Brain Res 833:291–296.

Parsey RV, Oquendo MA, Simpson NR, Ogden RT, Van Heertum R, Arango V, Mann JJ (2002) Effects of sex, age, and aggressive traits in man on brain serotonin 5-HT$_{1A}$ receptor binding potential measured by PET using [C-11]WAY-100635. Brain Res 954:173–182.

Parsey RV, Ogden RT, Miller JM, Tin A, Hesselgrave N, Goldstein E, Mikhno A, Milak M, Zanderigo F, Sullivan GM, Oquendo MA, Mann JJ (2010) Higher serotonin 1A binding in a second major depression cohort: modeling and reference region considerations. Biol Psychiatry 68:170–178.

Passchier J, van Waarde A (2001) Visualisation of serotonin-1A (5-HT$_{1A}$) receptors in the central nervous system. Eur J Nucl Med 28:113–129.

Passchier J, van Waarde A, Vaalburg W, Willemsen AT (2001) On the quantification of [^{18}F]MPPF binding to 5-HT$_{1A}$ receptors in the human brain. J Nucl Med Off Publ Soc Nucl Med 42:1025–1031.

Paxinos G, Watson C, Petrides M, Rosa M, Tokuno H (2011) The marmoset brain in stereotaxic coordinates, 1st edition. London; Waltham, MA: Academic Press.

Pazos A, Palacios JM (1985) Quantitative autoradiographic mapping of serotonin receptors in the rat brain. I. Serotonin-1 receptors. Brain Res 346:205–230.

Pike VW, McCarron JA, Lammertsma AA, Osman S, Hume SP, Sargent PA, Bench CJ, Cliffe IA, Fletcher A, Grasby PM (1996) Exquisite delineation of 5-HT$_{1A}$ receptors in human brain with PET and [carbonyl-^{11}C]WAY-100635. Eur J Pharmacol 301:R5–7.

Plenevaux A, Weissmann D, Aerts J, Lemaire C, Brihaye C, Degueldre C, Le Bars D, Comar D, Pujol J, Luxen A (2000) Tissue distribution, autoradiography, and metabolism of 4-(2'-methoxyphenyl)-1-[2' -[N-2"-pyridinyl)-p-[(18)F]fluorobenzamido] ethyl]piperazine (p-[(18)F]MPPF), a new serotonin 5-HT(1A) antagonist for positron emission tomography: An In vivo study in rats. J Neurochem 75:803–811.

Portas CM, Bjorvatn B, Fagerland S, Grønli J, Mundal V, Sørensen E, Ursin R (1998) On-line detection of extracellular levels of serotonin in dorsal raphe nucleus and frontal cortex over the sleep/wake cycle in the freely moving rat. Neuroscience 83:807–814.

Python A, Steimer T, de Saint Hilaire Z, Mikolajewski R, Nicolaidis S (2001) Extracellular serotonin variations during vigilance states in the preoptic area of rats: a microdialysis study. Brain Res 910:49–54.

Rabiner EA, Messa C, Sargent PA, Husted-Kjaer K, Montgomery A, Lawrence AD, Bench CJ, Gunn RN, Cowen P, Grasby PM (2002) A database of [(11)C]WAY-100635 binding to 5-HT(1A) receptors in normal male volunteers: normative data and relationship to methodological, demographic, physiological, and behavioral variables. NeuroImage 15:620–632.

Seeman P, Kapur S (2003) Anesthetics inhibit high-affinity states of dopamine D2 and other G-linked receptors. Synapse 50:35–40.

Shouse MN, Staba RJ, Saquib SF, Farber PR (2000) Monoamines and sleep: microdialysis findings in pons and amygdala. Brain Res 860:181–189.

Shrestha S, Hirvonen J, Hines CS, Henter ID, Svenningsson P, Pike VW, Innis RB (2012) Serotonin-1A receptors in major depression quantified using PET: controversies, confounds, and recommendations. NeuroImage 59:3243–3251.

Shrestha SS, Liow J- S, Lu S, Jenko K, Gladding RL, Svenningsson P, Morse CL, Zoghbi SS, Pike VW, Innis RB (2014) (11) C-CUMI-101, a PET radioligand, behaves as a serotonin 1A receptor antagonist and also binds to α(1) adrenoceptors in brain. J Nucl Med 55:141–146.

Sibon I, Benkelfat C, Gravel P, Aznavour N, Costes N, Mzengeza S, Booij L, Baker G, Soucy J- P, Zimmer L, Descarries L (2008) Decreased [^{18}F]MPPF binding potential in the dorsal raphe nucleus after a single oral dose of fluoxetine: a positron-emission tomography study in healthy volunteers. Biol Psychiatry 63:1135–1140.

Skinbjerg M, Sibley DR, Javitch JA, Abi-Dargham A (2012) Imaging the high-affinity state of the dopamine D2 receptor in vivo: fact or fiction? Biochem Pharmacol 83:193–198.

Stiedl O, Pappa E, Konradsson-Geuken Å, Ögren SO (2015) The role of the serotonin receptor subtypes 5-HT$_{1A}$ and 5-HT$_7$ and its interaction in emotional learning and memory. Front Pharmacol 6:162.

Tauscher J, Bagby RM, Javanmard M, Christensen BK, Kasper S, Kapur S (2001) Inverse relationship between serotonin

5-HT(1A) receptor binding and anxiety: a [(11)C]WAY-100635 PET investigation in healthy volunteers. Am J Psychiatry 158:1326–1328.

van Goethem NP, Schreiber R, Newman-Tancredi A, Varney M, Prickaerts J (2015) Divergent effects of the "biased" 5-HT_{1A} receptor agonists F15599 and F13714 in a novel object pattern separation task. Br J Pharmacol 172:2532–2543.

Whittington RA, Virág L (2006) Isoflurane decreases extracellular serotonin in the mouse hippocampus. Anesth Analg 103:92–98, table of contents.

Wooten DW, Moraino JD, Hillmer AT, Engle JW, Dejesus OJ, Murali D, Barnhart TE, Nickles RJ, Davidson RJ, Schneider ML, Mukherjee J, Christian BT (2011) In vivo kinetics of [F-18]MEFWAY: a comparison with [C-11]WAY100635 and [F-18]MPPF in the nonhuman primate. Synapse 65:592–600.

Yokoyama C, Kawasaki A, Hayashi T, Onoe H (2013) Linkage between the midline cortical serotonergic system and social behavior traits: positron emission tomography studies of common marmosets. Cereb Cortex 1991 23:2136–2145.

Yokoyama C, Onoe H (2015) Positron emission tomography imaging of the social brain of common marmosets. Neurosci Res 93:82–90.

Yokoyama C, Yamanaka H, Onoe K, Kawasaki A, Nagata H, Shirakami K, Doi H, Onoe H (2010) Mapping of serotonin transporters by positron emission tomography with [^{11}C]DASB in conscious common marmosets: comparison with rhesus monkeys. Synapse 64:594–601.

Zimmer L, Fournet G, Benoît J, Guillaumet G, Le Bars D (2003) Carbon-11 labelling of 8[[3-[4-(2-[(11)C]methoxyphenyl) piperazin-1-yl]-2-hydroxypropyl]oxy]thiochroman, a presynaptic 5-HT(1A) receptor agonist, and its in vivo evaluation in anaesthetised rat and in awake cat. Nucl Med Biol 30:541–546.